



HAL
open science

Optimized total order for mathematical morphology on metric spaces

Emmanuel Chevallier, Jesus Angulo

► **To cite this version:**

Emmanuel Chevallier, Jesus Angulo. Optimized total order for mathematical morphology on metric spaces. 2014. hal-00948232v2

HAL Id: hal-00948232

<https://hal.science/hal-00948232v2>

Preprint submitted on 19 Mar 2014 (v2), last revised 15 Jan 2015 (v3)

HAL is a multi-disciplinary open access archive for the deposit and dissemination of scientific research documents, whether they are published or not. The documents may come from teaching and research institutions in France or abroad, or from public or private research centers.

L'archive ouverte pluridisciplinaire **HAL**, est destinée au dépôt et à la diffusion de documents scientifiques de niveau recherche, publiés ou non, émanant des établissements d'enseignement et de recherche français ou étrangers, des laboratoires publics ou privés.

Optimized total order for mathematical morphology on metric spaces

Emmanuel Chevallier, Jesús Angulo

CMM-Centre de Morphologie Mathématique, MINES ParisTech; France
`emmanuel.chevallier@mines-paristech.fr`

October 2013

Abstract

In this paper, we discuss the problem of total ordering for mathematical morphology. The study is focused on color and DTI images, but results are valid in any metric space. The discontinuities issue of total orders has already been evoked in mathematical morphology, but remains rarely studied. This phenomenon is highlighted and formalised in this paper. We propose a novel approach to avoid discontinuities based on a recursive algorithm. The key point of the proposed method is to adapt the order to the studied image. The proposed framework presents invariance to isometric transformations of the color space. Promising results are presented.

1 Introduction

Since its apparition in the sixties, mathematical morphology has become one of the major theory of nonlinear image processing. Originally used for binary images [6], the theory has followed the technical evolution of computer science which has enabled the manipulation of more and more complex images [12]. The set theory was sufficient to study binary images. However, the apparition of gray-scale images required the introduction of the notion of order. The theory of mathematical morphology is now fully based on the lattice theory [13, 9]. The case where the value space is endowed with a total order is the most comfortable framework for morphological processing. However, if it is natural to endow gray-scale images with a total order, it is more difficult when the pixel values do not have an unidimensional structure [14]. Indeed, we show that the information contained in a total order is

too weak to completely represent the value space. In many situations, one prefers to use partial order such as product orders on vector spaces. Using a product order is equivalent to processing components independently. The order structure becomes natural but we lose some information about the geometry of the original value space. Both choices present a loss of information. However, while partial orders are widely studied and used in mathematical morphology, the study of total orders remains mainly limited to lexicographic orders [3, 2, 8].

The interest of product orderings in mathematical morphology is still subject of recent research [7, 4], mainly by considering the geometric and invariant properties of the underlying space. Other recent works on partial ordering for morphological operators on vector images were motivated by the need of taking into account some prior information about how to order vectors: either to learn the order from training samples [16] or to build the order according to the outlieriness distribution [17]. Therefore, partial ordering can become image adaptive and consequently leads to more relevant morphological operators.

Since the apparition of multivariate images, very few papers have addressed the problem of total orders in a general way [5] [10]. As we discuss in the first part of the paper, previous approaches of total ordering focussed exclusively on building a regular ordering on the value space of the image, without taking into account how the corresponding values were located on the image support. The aim of this paper is to introduce a total ordering which is adapted to each image according to both the position of the values on the space and the location of these values on the image support. One can therefore consider our approach as an image adapted total ordering. We formulate this task as an optimization problem which cannot be solved using classical optimization techniques. Thus, we introduce an hierarchical recursive algorithm aiming at finding a possible solution.

2 Notations and recalls

We set here a few notations and remind elementary operators of mathematical morphology [12, 15]. Let us consider an image I as a function:

$$I : \begin{cases} \Omega \rightarrow \mathcal{V} \\ p \mapsto I(p) \end{cases}$$

where Ω is the support space of pixels p : typically $\Omega \subset \mathbb{Z}^2$ or \mathbb{Z}^3 for discrete images. The pixel values of the image belong to the space \mathcal{V} . Typically we

have $\mathcal{V} \subset \mathbb{R}$ for grey-scale images, $\mathcal{V} \subset \mathbb{R}^n$ for multivariate vector images, or $\mathcal{V} \subset \mathcal{M}$ for manifold valued images. In this paper, we address images where \mathcal{V} is any metric space. Points in \mathcal{V} will be generally called colors. We denote by $I(\Omega) \subset \mathcal{V}$ the set of colors of \mathcal{V} presented in the image $I(p)$.

Unlike linear processing mainly based on linear convolution (i.e., weighting averaging), mathematical morphology is based on sup and inf-convolution. The choice of the convolution kernel offers a range of processing. Thus, the two basic operators of mathematical morphology on are the erosion and the dilation of an image $I(p)$, $I : \Omega \rightarrow \mathbb{R}$, by $B \subset \Omega$ given respectively by: $\varepsilon_B(I)(p) = \inf_{q \in B(p)}(I(q))$ and $\delta_B(I)(p) = \sup_{q \in B(p)}(I(q))$, where the set B defines the structuring element (the equivalent of the convolution kernel) and $B(p)$ defines the neighbourhood of p according to the shape of B . Note that here we only focuss on flat structuring elements. Other morphological filters, such as the opening $\gamma_B(I)$ and closing $\varphi_B(I)$, are obtained by composition of dilation and erosion; i.e, $\gamma_B(I) = \delta_B(\varepsilon_B(I))$ and $\varphi_B(I) = \varepsilon_B(\delta_B(I))$. More evolved filters and transforms are obtained from composition of openings/closings. Another nonlinear operator also based on ordering, which is particularly useful in image denoising, is the median filter: $m_B(I)(p) = \text{med}_{q \in B(p)}(I(q))$.

3 Existing total orders

The problem of total ordering for multivariate images is a relatively well known problem in mathematical morphology. The essential difficulty is that the topology induced by a total order on a multidimensional space can not reproduce the natural topology of the vector space. Arising as a milestone limitation, we have the following lemma.

Lemma 3.1 *Let (X, d) be a metric space endowed with a total order \leq . Suppose that there exist a positive real number R and three points $x_1, x_2, x_3 \in X$ such that the three balls $B(x_i, R+1)$ are disjoint and such that the complementary $B^C(x_i, R+1)$ of each ball $B(x_i, R+1)$ is connected, as in Fig. 1. Then for all $r > 0$, there exist three points a, b and c in X such that*

$$\begin{cases} a \leq b \leq c, \\ d(a, b) \geq R, \\ d(a, c) \leq r. \end{cases}$$

Proof. We can assume that $x_1 < x_2 < x_3$. We argue by contradiction and assume that there exists $r > 0$ such that for all $a, b, c \in X$ one at least of the three above conditions doesn't hold. It follows that $a \leq b$, $d(a, b) \geq R$

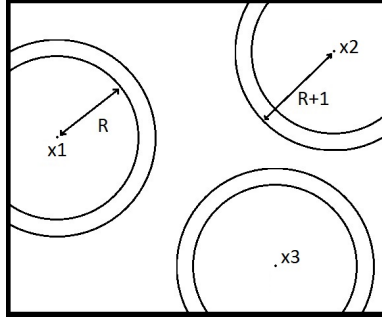


Figure 1: The metric space X is here a rectangle of the Euclidean plan

and $d(a, c) \leq r$ imply $c < b$. Without loss of generality we can assume that $r \leq 1$. Consider the set E of points a in $B^C(x_2, R + 1)$ such that $a \leq x_2$. We recall the following property: let A be an open and close subset of the connected set B . Then $A = \emptyset$ or $A = B$. We use this assertion with $A = E$ and $B = B^C(x_2, R + 1)$ to exhibit a contradiction. If a point a is in E then all the points in $B(a, r) \cap B^C(x_2, R + 1)$ are in E . If a point $c \in B^C(x_2, R + 1)$ is not in E then the ball $B(c, r)$ cannot contain a point a with $a \leq x_2$ because all points $x \in B(a, r)$ would satisfied $x \leq x_2$. It follows that E is an open and close subset of $B^C(x_2, R + 1)$. The point x_1 is in E : E is a non-empty set. The connectivity of $B^C(x_2, R + 1)$ implies that $E = B^C(x_2, R + 1)$, a contradiction with $x_3 > x_2$.

This lemma tells us that for any total order, functions $\sup(x, y) : \mathbb{R}^n \times \mathbb{R}^n \rightarrow \mathbb{R}^n$ and $\inf(x, y)$ present high irregularities. This result has strong negative implications. Given a total order, it is always possible to find an image where the erosion and dilation are highly irregular in local neighborhoods.

An illustration of this phenomenon is given by the following toy example Fig. 2. The image is composed by 3 different colors. The black is mainly composed of $a = (0, 0, 0)$ with a few pixels $b = (0.1, 0, 0)$. The blue is represented by $c = (0, 0, 1)$. According to the lexicographic ordering, we are precisely in the situation described in the lemma. Fig. 2 shows us the result of a 1×1 square dilation.

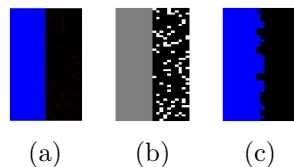


Figure 2: (a): Original image, (b): Projection on the lexicographic order, (c): Lexicographic dilation

the representation space. In the ideal case, morphological operator should be invariant to this operation. If distances in the representation space still represent distances between objects after the change of coordinates, this operation must be isometric or at least homothetic. Thus, morphological operators should be invariant to isometric transformations. We think that in most cases, the only criterion that an order has to respect for mathematical morphology is the preservation of neighbourhood and distances. Arising as a result, the order has then to be based only on the topological structure of the representation space.

4 An order adapted to a given image

4.1 Motivation

As we have discussed above, it is not possible to create a total order that preserves neighbourhood on a multidimensional space. The philosophy of [5][10] is to try to minimize the difference between spatial neighbourhoods and neighbourhoods in the space of order. However it is possible to push this idea further. Even for the best total order in the sense of the measure previously defined, our Lemma tells us that the processing of a particular image can give highly irregular results. As a consequence, it might be more interesting to look for the best order, being given an image, than to look for the best order in general. Indeed, restricting the evaluation of a total order to a particular image, largely enhance the potential quality of the order. An order on a multidimensional space can present important discontinuities that might not affect the processing of a particular image. Firstly the evaluation of a total order given a specific image only gives importance to colors that lay in the image. Indeed, no other colors are introduced by flat erosion or dilation. Decreasing the size of the set to be ordered often enables to find total orders way more regular. More precisely, it becomes much easier to find orders that avoid having two points close in the color space and far in the order. Secondly, this situation can be tolerated to the extend that colors do not always appear in same structuring element. For instance if two colors never appear in the same structuring element, their relative positions in the order has no impact on the quality of the process.

We agree with [5] on the fact that if points are close in the color space, they should remain close in the order. However, we think the reverse is not always necessary. Let us consider a binary image represented on the real line, where black and white are not represented by 0 and 1 but 0 and 10. In this situation there are two points close in the order chain and distant

regarding the metric of the color space. However, this does not introduce any irregularity in the morphological operators.

In order to transpose this topological intuition of “closeness in color space implied closeness in the order”, specially where the involved colors are near on the image support space, we introduce a cost function to be minimised by the total ordering.

4.2 Cost function

Given an image, we would like to define a new cost function that measure the quality of the order regarding rank based operators. We first need to clarify what criterion has to be respected. Let a and b be two close colors according to a given metric distance $d(a, b)$ in \mathcal{V} . Let c be a third color far from a and b . Let us define a notion of co-occurrence of colors:

$$C_I(a, b) = \text{Card}\{p \in \Omega, \exists q \in B(p), (I(p), I(q)) \in \{(a, b), (b, a)\}\} \quad (1)$$

If $C_I(a, c)$ or $C_I(b, c)$ is reasonably small, no irregularities will be created by the colors a, b, c . If $C_I(a, c)$ and $C_I(b, c)$ are significant, it is important that $a < c \Leftrightarrow b < c$.

The computation of co-occurrences involves that one has fixed a typical size/shape of the structuring element which will be used in subsequent processing. Let consider we have endowed $I(\Omega)$ with a total ordering \leq . We can define the following quantity:

$$P(I) = \sum_{\substack{a, b, c \in I(\Omega), \\ a < c < b}} (f(d(c, a), d(c, b), d(a, b)) \cdot C_I(c, a) \cdot C_I(c, b) \cdot C_I(a, b)), \quad (2)$$

where $f(\cdot, \cdot, \cdot)$ is an increasing function of its two first variables and decreasing according to the third variable.

Given an image $I(p)$, this adapted cost function is more tolerant for some specific orders than the cost function defined in [5]. Cost function $P(I)$ has been designed to represent as well as possible what is expected of an order. However, as a standard image often contains more than ten thousand different colors, this cost function presents the serious drawback of not being computable. Thus, given two orders, it is difficult to compare them using this cost function. One of the main role of this cost is to show that what is required from an order is much weaker than what is required in [5]. However, it is possible to try to minimize this cost function using a recursive procedure, without computing globally the cost of the full set of points. It might not be possible to compare explicitly the cost of the

bit-mixing paradigm or the Peano curve with the cost of an order obtained by the following algorithm. Nevertheless, we expect it to be much lower due to its construction.

5 Minimisation of the cost function

5.1 Overview of the algorithm

Here are the main steps of the algorithm.

- Perform a clustering of the data $I(\Omega)$ in a given number of clusters: $\{Cluster_i\}_{1 \leq i \leq n}$.
- Compute the following quantities,
 - Minimum distances between clusters: $D(i, j)$, $1 \leq i, j \leq n$,
 - Co-occurrence of clusters in different structuring elements: $C(i, j)$, $1 \leq i, j \leq n$.
- Order the n clusters according to $C(i, j)$, $D(i, j)$, and the corresponding cost function P . The point of the clustering is to make this operation possible by reducing the number of parameters of the minimization. If $Cluster_i < Cluster_j$ we impose that $\forall (c_k, c_l) \in Cluster_i \times Cluster_j$ involves $c_k < c_l$.
- Perform the same procedure recursively on each cluster.
- After a given threshold, stop the recursion. For each cluster, order all its points according to a criterion based on distances to previous and next clusters.

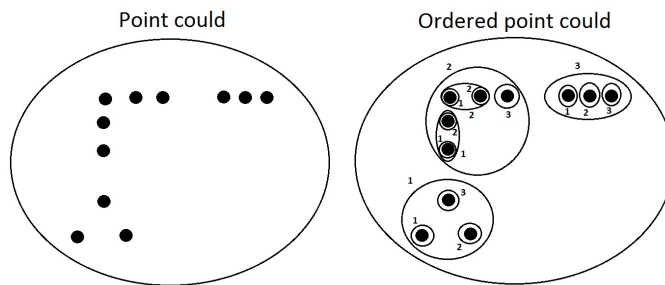


Figure 4: The point cloud is recursively ordered

In this short description we did not mention a significant issue which makes the algorithm a bit complicated. When the recursive procedure is

applied to $Cluster_i$, one has to take into account the result of the ordering from other clusters. Indeed, at the first step of the recursion, nothing has to be taken into account outside of the considered set of colors $\{I(\Omega)\}$. However, contrary to global set $\{I(\Omega)\}$, $Cluster_i$ can no longer be considered as isolated from the rest of color values. If there exist colors c_k in $Cluster_i$ and colors c_l in $Cluster_j$ such that $d(c_k, c_l)$ is small, then it is not possible to order $Cluster_i$ without taking into account $Cluster_j$. To order $Cluster_i$, one needs to know the set of its neighbour clusters and their relative ordering. These are the main ingredients to the recursive function. For the first iteration, the recursive function is called with a unique cluster without neighbours.

The recursive function *funt_recursive*, take the following arguments: an image I , a set of cluster $S_1 = \{Cluster_i\}$ from $\{I(\Omega)\}$, a total order on this set of clusters $<_1$, the index of a specific cluster *index*, and a number that represents the level of recursion *depth*. S'_1 will denote $S_1 \setminus Cluster_{index}$. Then *funt_recursive* returns an order on $Cluster_{index}$.

If *depth* is lower than a given threshold:

- For each cluster $Cluster_i$ find the point c_k in $Cluster_{index}$ that minimizes the distance to $Cluster_i$. If $i = index$, let c_k be the barycentre of $Cluster_{index}$.
- Set $\{c_k\}$ is completed with random points in $Cluster_{index}$ to reach minimum number of points. Perform a clustering of $Cluster_{index}$ using a k-means algorithm initialized with the c_i . Let $S_{Cluster_{index}}$ be this new set of clusters.
- Let us consider the set S_2 of clusters composed of clusters in S'_1 , and clusters created during the previous instruction. $S_2 = S'_1 \cup S_{Cluster_{index}}$. Compute D , the minimum distances between pairs of clusters of S_2 and C , the co-occurrence of pairs of clusters in I .
- Perform a minimization of P on S_2 , using C and D , such that the new total order $<_2$ is compatible with $<_1$. If $Cluster_i$ and $Cluster_j$ are in S , $(Cluster_i <_1 Cluster_j) \Rightarrow (Cluster_i <_2 Cluster_j)$. Furthermore, for $Cluster_i$ in $S_{Cluster_{index}}$ and $Cluster_j$ in S'_1 , $Cluster_i <_2 Cluster_j \Leftrightarrow Cluster_{index} <_1 Cluster_j$. The situation is summarized in Fig. 5.
- Initialize an empty array *total_order*.
- For each cluster in $S_{Cluster_{index}}$, taken successively according to $<_2$:

- Select a set S_3 of neighbour clusters in the set S_2 , in terms of co-occurrence. The current cluster is part of S_3 .
- Let $<_3$ be the order induced on S_3 by the $<_2$.
- Then $total_order = total_order$ concatenated with the output of $funt_recursive$, which is called with the following arguments: I , S_3 , $<_3$, the index of the current cluster and $depth + 1$.

If $depth$ equals the given threshold:

- Compute the minimal distances between each pair of clusters.
- Select in S the nearest neighbour of $Cluster_{index}$ greater than $Cluster_{index}$ and the nearest neighbour lower than $Cluster_{index}$.
- Order elements of $Cluster_{index}$ according to their distance to the two clusters selected during the previous step.

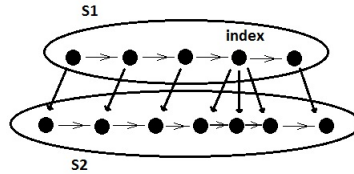


Figure 5: Construction of $<_2$ (see description of the algorithm).

5.2 Optimization over the permutation space

We note that, according to this algorithm the set to be ordered is no longer the set of all colors present in the image, but the set of clusters S at each level of recursion. The cost function P can be calculated if the cardinal n of S is reasonable. If the set S does not exceed $n = 10$ elements, it is conceivable to calculate the cost of all the permutations and select the one associate to the order which minimizes P . However, this solution requires an important computation time. An alternative solution consists in optimizing the cost function iteratively. It is well know that from a permutation it is possible to reach any other permutation by composing transpositions. Given a permutation, we select the transposition that minimize the cost function, and we repeat the process until we fall in a minima. As we do not know whether the cost function has any convex property, the minima might only be a local minima. However, under $n = 10$ elements it is possible to compare the results with the global exploration. In all tested situations with $n = 10$ elements, the optimization by transposition did not fall in a local minima.

6 Order invariance

Cost function $P(I)$ does not depend on coordinates of colors but only on their mutual distances and their co-occurrences. As the notion of co-occurrences remains unchanged under bijective transformations, the cost $P(I)$ is invariant to any isometric transformation. However, the choice of a particular function $f(\cdot, \cdot, \cdot)$ can induce larger class of invariance. For instance the following cases:

$$f(d(c, c_i), d(c, c_j), d(c_i, c_j)) = \frac{d(c, c_i) + d(c, c_j)}{d(c_i, c_j)}, \quad (3)$$

or

$$f(d(c, c_i), d(c, c_j), d(c_i, c_j)) = \frac{d(c, c_i)d(c, c_j)}{d(c_i, c_j)^2}, \quad (4)$$

also provides invariance of $P(I)$ to homothetic transformations. We can also note that for the function:

$$f(d(c, c_i), d(c, c_j), d(c_i, c_j)) = \frac{d(c, c_i)d(c, c_j)}{d(c_i, c_j)}, \quad (5)$$

homothetic transformations simply result in the multiplication of $P(I)$ by a positive constant. Consequently, as the notion of minimum is invariant under increasing transformation, the minimization of $P(I)$ should remain relatively stable.

If T is an isometric (or homothetic) transformation of the value space \mathcal{V} , and Φ a morphological operator $\{\Omega, \mathcal{V}\} \rightarrow \{\Omega, \mathcal{V}\}$, then T and Φ commutes for any image I , i.e.,

$$\Phi(T(I)) = T(\Phi(I)).$$

7 Results of morphological image processing

As we just discussed, explicit calculation of P is not possible for standard images. Exact comparison between orders produced by our minimization and classical lexicographic order or bit-mixing order proposed in [5] is unfortunately not possible. At the first step of the recursion, the initial set Ω is divided into n clusters, with n reasonably small. Assimilating clusters and centroids enables us to order them according to the lexicographic or the bit-mixing paradigm. It is then possible to compare the cost of each order by computing the corresponding values P on the set of centroids. This parameter is computed to obtain a quantitative comparison of the three orders.

In every examples, the minimization is launched with the following parameters:

- Function f corresponds to model (4):

$$f(d(c, c_i), d(c, c_j), d(c_i, c_j)) = \frac{d(c, c_i) \times d(c, c_j)}{d(c_i, c_j)^2};$$

- The set S is divided into $n = 10$ clusters;
- We stop the recursion when $depth = 2$.

7.1 Colour imaging

We present results obtained for two different RGB color images. The first one is a microscopic blood vessel from a fluoresce microscope, the second one is a natural image. For both of them we have minimized P using the recursive algorithm discussed in previous section. The distance $d(c_i, c_j)$ between colors is the Euclidean distance of the RGB color space.

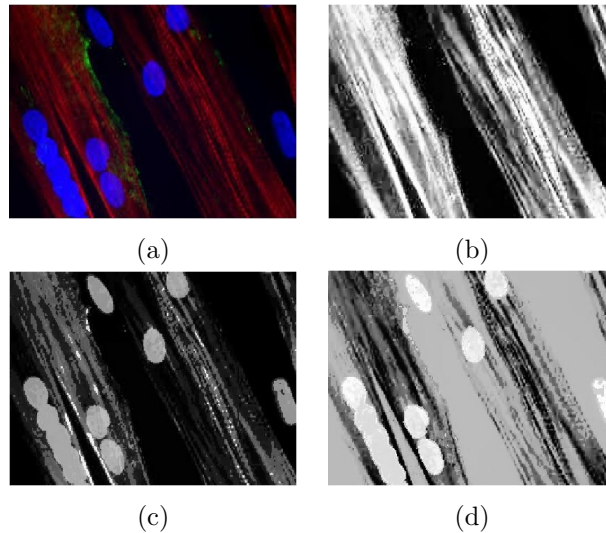


Figure 6: Projection of the total order on the image support: (a) original RGB image $I(p)$; (b) lexicographic order; (c) bit-mixing order; (d) our image adapted total order.

Fig. 6 represents the RGB color image together with the projection of the total order on the image support for the three cases of total order. As we can see, the blue spots are totally invisible to the lexicographic ordering. Note that the lexicographic ordering starts by red, then green and finally blue. The bit-mixing paradigm and the image adapted total order gives different results but are both coherent with the original image.

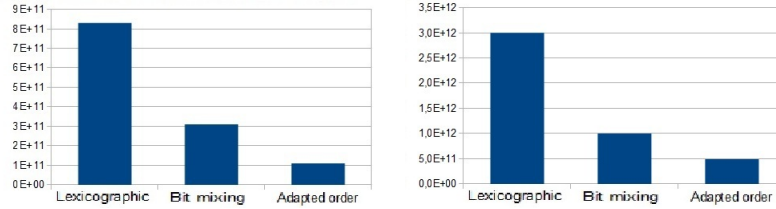


Figure 7: Evaluation of the cost function P at the first step of the recursion: (a) image $I(p)$ from Fig. 6, (b) image $I(p)$ from Fig. 9.

Using now each total ordering, we can compute morphological color operators. Fig. 8 gives the corresponding openings and closing using as structuring element a square of 7×7 pixels. As expected the lexicographic ordering produces important discontinuities around the blue spots. The bit-mixing paradigm and image adapted total order gives different results but both preserve the regularity of boundaries. Besides the visual comparison of these results, we compare the cost P at the first step of the recursion for each order, which for the current example are given in Fig. 7(a), which are coherent with the visual results.

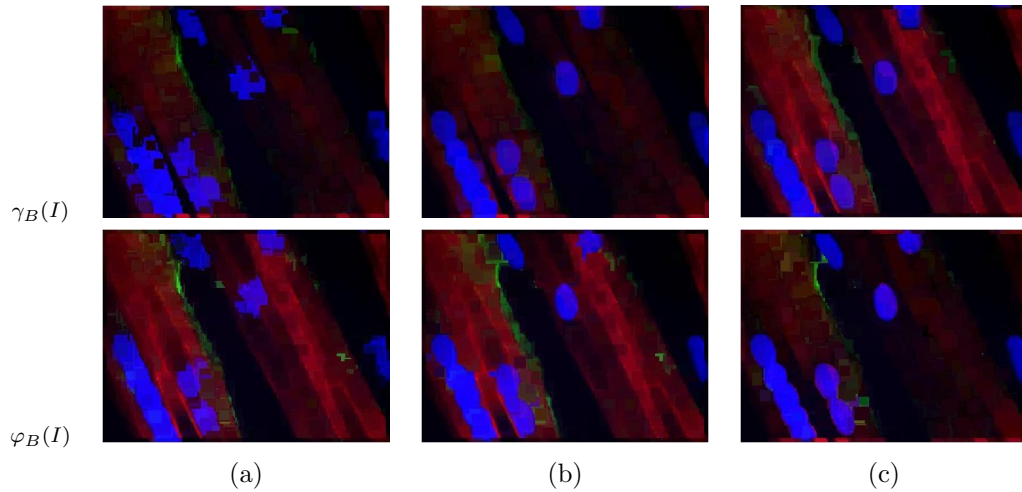


Figure 8: Morphological processing of image from Fig. 6, top row, opening $\gamma_B(I)$ and bottom row, closing $\varphi_B(I)$ using lexicographic order in (a), bit-mixing order in (b) and our image adapted total order in (c). Structuring element is B is a square of 7×7 pixels

For the second studied example, we applied the same approach. Fig. 9 provides the original RGB image and the image representation of the three

orders. Unlike to the previous example, the lexicographic order is able to distinguish all interesting objects of the image. Furthermore, it seems to give an order smoother than the bit-mixing paradigm and the image adapted total order. However this visual impression is not corroborated by the computation of the cost P , see Fig. 7(b).

In fact, as we can observe from the opening/closing operators depicted in Fig. 10, the regularity of the grey-scale projection on lexicographic order is only an illusion. Both lexicographic order and the bit-mixing order present high discontinuities on blue and yellow boundaries. On this example, our image adapted total order is the only one of the three orders that provides satisfying results in terms of regularity for the opening and closing.

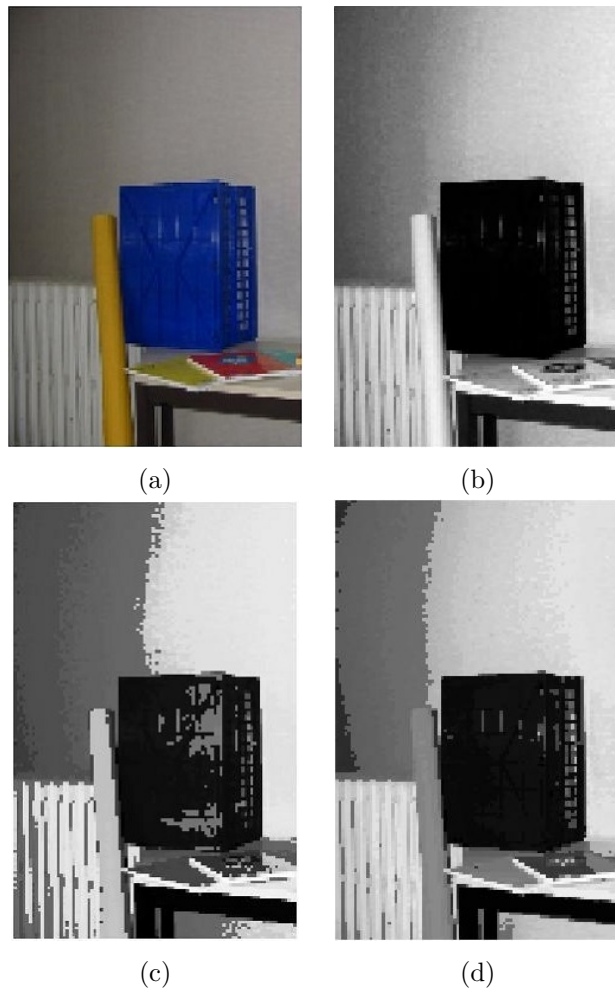


Figure 9: Projection of the total order on the image support: (a) original RGB image $I(p)$; (b) lexicographic order; (c) bit-mixing order; (d) our image adapted total order.

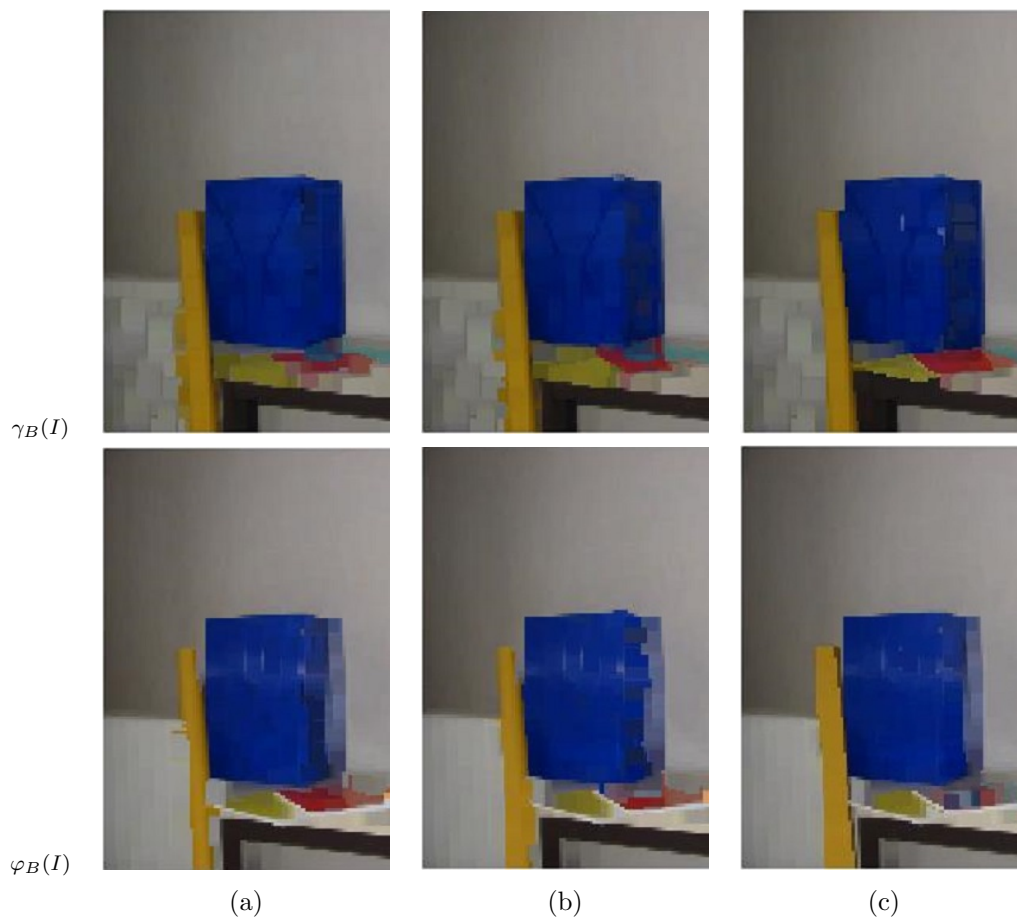


Figure 10: Morphological processing of image from Fig. 9, top row, opening and bottom row, closing using lexicographic order in (a), bit-mixing order in (b) and our image adapted total order in (c). Structuring element is B is a square of 7×7 pixels.

7.2 Diffusion Tensor Imaging

We try here to compare the morphological processing associated to lexicographic orders, the bit-mixing paradigm and the image adapted total order. We recall that in DTI, each pixel of the image contains a symmetric positive definite matrix of size 3×3 , $\text{SPD}(3)$. As the matrix is symmetric, it can be parametrized by the 6 upper-diagonal coefficients:

C1	C2	C3
	C4	C5
		C6

Figure 11: Standard parametrization of a symmetric matrix

A matrix of $SPD(3)$ can be represented as an ellipsoid. A DTI image can be visualized using ellipsoids:

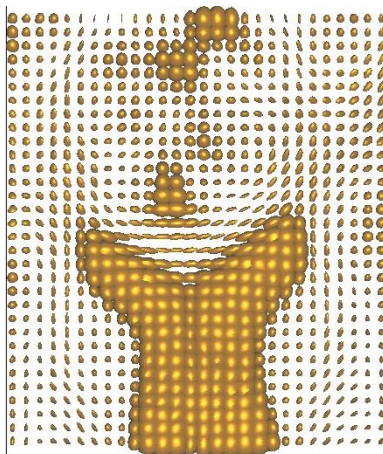


Figure 12: DTI image

This parametrization induce a lexicographic order on $SPD(3)$. This order is called *LEX1* in what follows. A second approach involves decomposing $SPD(n)$ matrices over rotations and eigenvalues. A symmetrical matrix can be diagonalized in an orthonormal basis. Then each $SPD(3)$ matrix can be represented by 3 eigenvalues and a rotation matrix. Using any angular representation of the rotation matrix, the $SPD(3)$ matrix can be represented by 3 eigenvalues 3 angles. Let us consider such a parametrization where the eigenvalues are sorted decreasingly. The associated lexicographic order is called *LEX2*.

The bit-mixing paradigm is applied on the first representation.

The image adapted total order is calculated according two metrics: the metric associated with the Frobenius scalar product, $\langle A, B \rangle = tr(AB^t)$, and the Log-Euclidean metric [18].

In every processing, the structuring element B is a square of 5×5 pixels
 Fig. 13 shows the result of openings for the different total orders

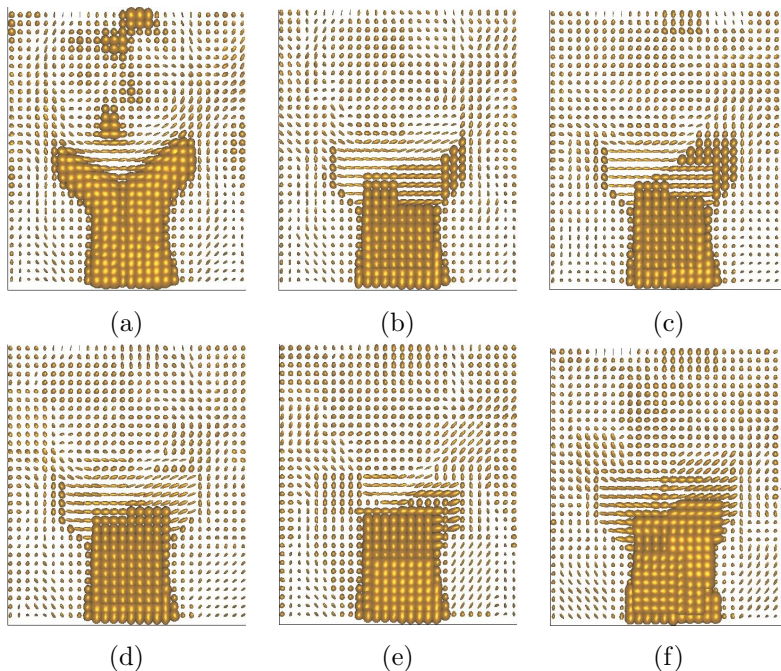


Figure 13: (original image in (a), and opening using $LEX1$ in (b), $LEX2$ in (c), bit-mixing paradigm in (d), image adapted total order using Frobenius norm in (e), and Log-Euclidean norm in (f))

Geodesic reconstruction using the different opening as marker are presented in Fig. 14

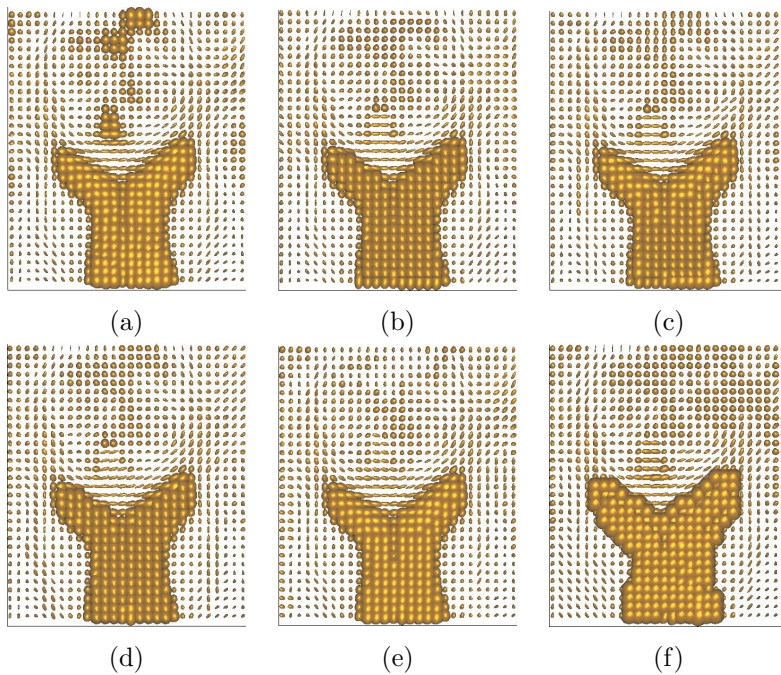


Figure 14: (original image in (a), and reconstruction using $LEX1$ in (b), $LEX2$ in (c), bit-mixing paradigm in (d), image adapted total order using Frobenius norm in (e), and Log-Euclidean norm in (f))

Fig. 15 shows the result of closings:

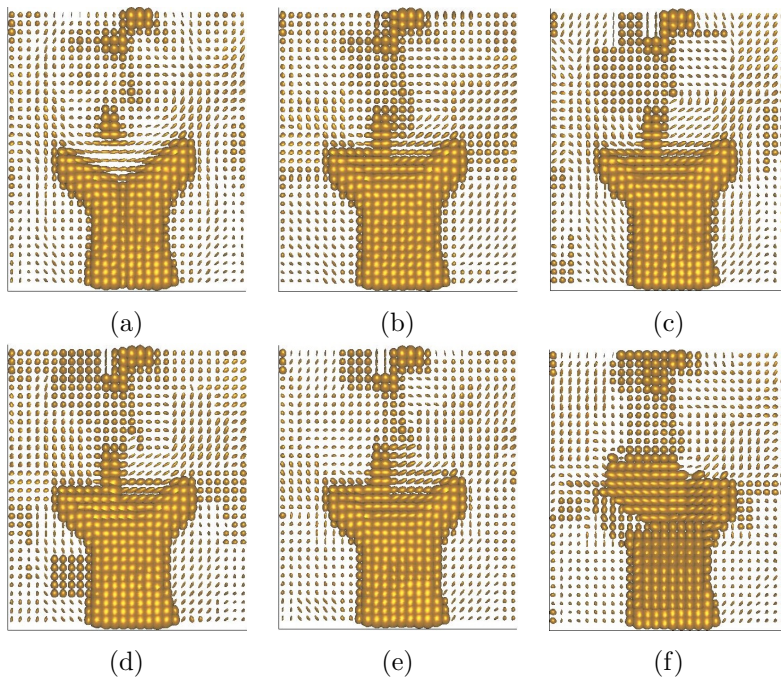


Figure 15: (original image in (a), and closing using $LEX1$ in (b), $LEX2$ in (c), bit-mixing paradigm in (d), image adapted total order using Frobenius norm in (e), and Log-Euclidean norm in (f))

Median filtering is presented in Fig. 16

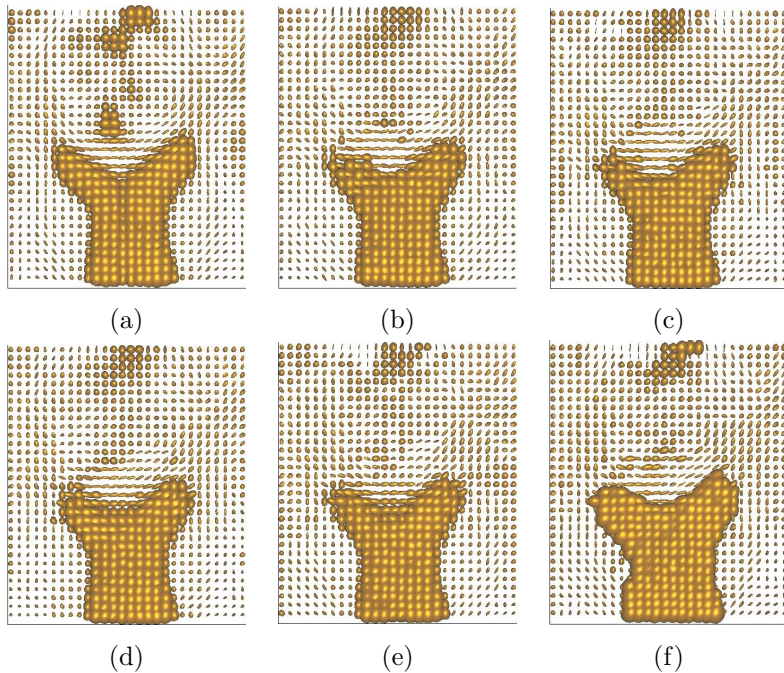


Figure 16: (original image in (a), and median using $LEX1$ in (b), $LEX2$ in (c), bit-mixing paradigm in (d), image adapted total order using Frobenius norm in (e), and Log-Euclidean norm in (f))

The image adapted total order does not always give better results than the lexicographic order or the bit-mixing paradigm, to the extent that the lexicographic and the bit-mixing do not always give bad results. However, the image adapted total order based on the Frobenius norm gives results at least as good as other orders, and better ones in several situations.

8 Conclusions and Perspectives

Despite the fact that no exact numerical quantification of the order regularities are brought, experimental results show the relevance of the proposed method. If it is not possible to prove the pertinence of a framework from only a limited set of examples. We can nevertheless conclude that on every tested images, the image adapted total order gives results at least as good as the lexicographic ordering or the bit-mixing paradigm.

On the one hand, our future research will intend to improve the algorithm of the minimization of the cost function. On the second hand, we will study the stability of the total order regarding modification of the studied image.

References

- [1] E. Aptoula and S. Lefvre. A Comparative Study on Multivariate Mathematical Morphology. *Pattern Recognition*, 40(11):2914–2929, 2007.
- [2] J. Angulo. Geometric algebra colour image representations and derived total orderings for morphological operators Part I: Colour quaternions. *Journal of Visual Communication and Image Representation*, 21 (1), 33-48, 2010.
- [3] J. Angulo. Morphological colour operators in totally ordered lattices based on distances. Application to image filtering, enhancement and analysis. *Computer Vision and Image Understanding*, 107(-3):56–73, 2007.
- [4] B. Burgeth, A. Kleefeld. Morphology for Color Images via Loewner Order for Matrix Fields. In *Mathematical Morphology and Its Applications to Signal and Image Processing (Proc. of ISMM'13)*, LNCS 7883, Springer, 243–254, 2013.
- [5] J. Chanussot, P. Lambert. Total ordering based on space filling curves for multivalued morphology. In *Proc. of fourth international symposium on Mathematical morphology and its applications to image and signal processing (ISMM '98)*, 51–58, 1998.
- [6] G. Matheron. *Random sets and integral geometry*. John Wiley & Sons, 1975.
- [7] J.J. van de Gronde, J.B.T.M. Roerdink. Group-Invariant Frames for Colour Morphology. In *Mathematical Morphology and Its Applications to Signal and Image Processing (Proc. of ISMM'13)*, LNCS 7883, Springer, 267–278, 2013.
- [8] A. Hanbury. Mathematical morphology in the HLS colour space. In *Proc. 12th British Machine Vision Conference (BMVC)*, Manchester, pp. II-451460, 2001.
- [9] H.J.A.M. Heijmans, C. Ronse. The algebraic basis of mathematical morphology - part I: Dilations and erosions. *Computer Vision, Graphics and Image Processing*, 50:245–295, 1990.
- [10] F. Florez-Revuelta. Ordering of the RGB space with a growing self-organizing network. Application to color mathematical morphology. In

Proc. of the 15th international conference on Artificial Neural Networks: biological Inspirations (ICANN'05), Part I, 385–390, 2005.

- [11] H. Sagan. *Space Filling Curves*, Springer-Verlag New-York, 1994.
- [12] J. Serra. *Image Analysis and Mathematical Morphology*, Academic Press, London, 1988.
- [13] J. Serra. *Image Analysis and Mathematical Morphology. Vol II: Theoretical Advances*, Academic Press, London, 1988.
- [14] J. Serra. Anamorphoses and function lattices. In (Dougherty ed.) *Mathematical Morphology in Image Processing*, 483–523, Marcel Dekker, N.Y., 1992.
- [15] P. Soille. *Morphological Image Analysis: Principles and Applications*, Springer-Verlag New York, 2003.
- [16] S. Velasco-Forero, J. Angulo. Supervised ordering in \mathbb{R}^n : Application to morphological processing of hyperspectral images. *IEEE Trans. Image Process.*, 20(11): 3301–3308, 2011.
- [17] S. Velasco-Forero, J. Angulo. Random projection depth for multivariate mathematical morphology. *IEEE Journal of Selected Topics in Signal Processing*, 6(7):753–763, 2012.
- [18] V. Arsigny, P. Fillard, X. Pennec Log-Euclidean metrics for fast and simple calculus on diffusion tensors. *Magnetic Resonance in Medecine*, 56:411-421, 2006.